In constructing dynamical equations to describe laser action it has been usually convenient to work with stationary modes. Following this here, we would interpret α and β accordingly and write from (2) equations for the β modes

$$\dot{n}_\beta = \Gamma_\beta[(N_1-N_2)n_\beta+N_1]-w_\beta n_\beta. \qquad (6)$$

Coupling these with other differential equations describing how relaxation processes change N_2 and N_1 in the material would give a set of equations analogous to those used to describe stimulated fluorescence.[6,7]

[6] A. L. Schawlow and C. H. Townes, Phys. Rev. 112, 1940 (1958).
[7] T. H. Maiman, Phys. Rev. 123, 1145 (1961).

However, unlike for fluorescence, when the fraction of incident photons which is scattered becomes large (as has been observed to be possible[2]) the transparency of the material to the incident radiation falls drastically. The resulting reduction in n_α reacts back on n_β through Γ_β and extra equations (of a form depending on special circumstances) describing n_α must be coupled to those above. The relations (1)–(6) also apply when either the incident, or scattered, or both waves (α and β) are boson waves (such as sound) other than light.

The author wishes to thank Morrel Cohen for stimulating discussions and the Aspen Institute of Humanities, Physics Division, for their hospitality during part of this work.

Charge Exchange and Dissociation of H⁺, H₂⁺, and H₃⁺ Ions Incident on H₂ Gas*

G. W. McClure

Sandia Laboratory, Albuquerque, New Mexico

A unified set of measurements has been conducted of the yield cross sections for the various fast charged and neutral atomic particles produced in single collisions of H⁺, H₂⁺, and H₃⁺ ions with H₂ gas molecules. The fast particles in question result from the dissociation or charge neutralization of the primary ions and have essentially the same velocity as the primary ions. The measurements cover the energy range from 3 to 100 keV for H⁺ primaries, 3 to 120 keV for H₂⁺ primaries, and 5 to 120 keV for H₃⁺ primaries. The yield cross sections of the various dissociation fragments of H₂⁺ and H₃⁺ primaries are found to vary as much as 20% with changes in ion source operating conditions. It is proposed that this variation is due to changes in the population of internal energy states of the primary ions. Results obtained for H₂⁺ primary ions are compared with the results of other investigators.

INTRODUCTION

THE destruction of fast H₂⁺ ions (10 to 100 keV kinetic energy) in collisions with H₂ molecules has been shown to occur partly by electron capture with conversion of the primaries to H₂ neutrals or H+H pairs and partly by electronic excitation leading to conversion of the primaries to H+H⁺ or H⁺+H⁺ pairs.[1–6] The heavy products of the primary ion destruction move within a few degrees of the direction of the primary ions and have essentially the same velocity as the primary ions.[7] By the use of detectors

such as the particle scintillation counter[4,5] and gas proportional counter,[6] these products are easily distinguishable from each other and are distinguishable from the relatively slow ionization and dissociation fragments of the target molecules. It is, therefore, possible to determine the production cross section for each of the particle types and, with some manipulation of detector apertures,[4] to determine the reaction cross sections for the various destruction modes of H₂⁺.

[1] K. K. Damodaran, Proc. Roy. Soc. (London) 239, 382 (1957).
[2] C. F. Barnett, Proceedings of the Second United Nations International Conference on the Peaceful Uses of Atomic Energy, Geneva, 1958 (United Nations, Geneva, 1958), Vol. 32, p. 398.
[3] N. V. Fedorenko, V. V. Afrosimov, R. N. Il'in, and D. M. Kaminker, Zh. Eksperim. i Teor. Fiz. 36, 385 (1959) [translation: Soviet Phys.—JETP 9, 267 (1959)].
[4] D. R. Sweetman, Proc. Roy. Soc. (London) A256, 416 (1960).
[5] J. Guidini, Compt. Rend. 253, 829 (1961).
[6] Albert Schmid, Z. Physik 161, 550 (1961).
[7] Dissociation fragments of primary ions of 5-keV kinetic energy are expected to appear at angles up to about 3° due to the mutual

repulsion of the dissociating particles when electronic transitions occur to antibonding states. The maximum angular divergence associated with this process should vary as the inverse ½ power of the primary ion energy. In some of the destructive collisions, a proton of the primary ion makes a nearly "head-on" impact with a proton of the target molecule. The first proton may then transfer a large fraction of its kinetic energy to the second and emerge from the collision at an angle much larger than that expected from the action of molecular antibonding forces. The cross section for these large-angle events can be roughly estimated from classical Rutherford scattering theory. Using the impulse approximation to the classical theory, the cross section for one of the protons of a 5-keV incident H₂⁺ ion to scatter more than 3° on an H₂ molecule is ≃1.6×10^{-17} cm². This is negligibly small compared to either the H₂ production cross section (≃10^{-15} cm²) or the dissociation cross section (≃5×10^{-16} cm²). Because of this circumstance, the "large-angle" collisions are usually ignored in accounting for the destruction of the primary ions.

The collision destruction of fast H$_2^+$ ions and the subsequent collisions of the fast destruction products play extremely important roles in high-voltage glow discharges in hydrogen gas. Fairly detailed discharge calculations based on existing cross-section data have been attempted,[8] but complete and dependable calculations must await the collection of more data on the heavy-particle-yield cross sections. There are indications that H$_3^+$ ions enter strongly in the mechanism of these discharges, but data on the modes of destruction of this species have been unavailable.

Much work remains to be done, both experimentally and theoretically, on hydrogen-ion collision cross sections in the energy range 10 to 100 keV. In this range the relative velocity of colliding systems is of the order of the orbital velocity of the bound electrons. Because of this circumstance, accurate theoretical calculations of inelastic cross sections are especially difficult.

The present work is a unified investigation of the production cross sections of both the charged and uncharged fast destruction fragments of H$_2^+$ and H$_3^+$ ions in the 5- to 100-keV energy range with H$_2$ as the target gas. A thin-window proportional counter is used as the detector of the collision products. The acceptance solid angle of the detector is sufficient to insure the collection of all of the fast secondaries produced at angles less than 2.2° relative to the primary beam. The present results augment previous data on H$_2^+$ destruction and provide the first available information on H$_3^+$ destruction.

All of the H$_2^+$ and H$_3^+$ cross sections are measured relative to the well-established cross section for electron capture by protons. The relative cross-section versus energy curve for this process is measured and fitted to existing absolute data to calibrate the apparatus and to provide assurance of the uniform sensitivity of the counter detector for protons of all energies between 3 and 120 keV. The H$_2^+$ experimental results are compared with the previous results of a number of other investigators, and sources of error in the various measurement techniques are discussed.

A preliminary investigation is made of the dependence of the measured H$_2^+$ and H$_3^+$ cross sections on the ion-source operating conditions. An "ion source effect" seems to be present which may account for unexplained discrepancies of the order of 20% among results of various investigators. This result uncovers an important new aspect in the interpretation of molecular-ion collision cross-section data.

APPARATUS

Hydrogen ions were generated in a cold cathode Penning discharge,[9] accelerated by a two-lens electro-static accelerator, and magnetically analyzed by deflection through an angle of 18°. Defining slits in the analyzer permitted H$^+$, H$_2^+$, and H$_3^+$ ions having an energy spread of 500 eV (this was the maximum spread expected from the 500 V operating potential of the source) to be completely separated for accelerator potentials greater than 3 kV. Over the entire range of energies studied, the energy resolution of the analyzer was greater than the energy spread due to the source. Hence, ions originating at various potential levels within the source could be selected for separate study.

The ion species selected by the analyzer was directed into the apparatus shown in Fig. 1 and collimated by defining apertures S$_1$ and S$_3$. The unscattered primary ion beam emergent from S$_4$ was deflected by plates D$_2$ into collector cup C$_3$ while the secondary ion beams produced by dissociation of the primary ions in T$_2$ were deflected into separate positions.[10] The neutral collision fragments H and H$_2$ from dissociation and charge neutralization of the primary ions proceed directly along the S$_1$-S$_3$ axis.

The beam current into cup C$_3$, measured by means of a vibrating reed electrometer, was of the order of 10^{-13} to 10^{-12} A. This unusually low level of beam current was needed in order that the detector not lose counts due to excessive count rates. Data runs were taken only after ascertaining that the loss of counts due to pulse-height analyzer dead time was less than 5%. A negatively biased ring around the entrance into C$_3$ insured that secondary electrons produced within the cup were turned back and a grounded shield surrounding C$_3$ prevented slow electrons originating outside the cup from causing a spurious contribution to the cup current.

The secondary atomic beams (comprising H only with H$^+$ primaries; H, H$_2$, and H$^+$ with H$_2^+$ primaries; and H, H$_2$, H$^+$, and H$_2^+$ with H$_3^+$ primaries) were detected by means of a counting apparatus consisting of entrance slit S$_5$, ionization chamber A, and additional elements shown in Fig. 2. The entire counter assembly swings as shown in Fig. 1, permitting the entrance slit S$_5$ to scan a curved area 0.963 in. wide and 8 in. long. A synchronous motor drive permitted any portion of this area to be scanned at a constant speed of 1 in./min while C$_3$ remained fixed to monitor the primary ion beam.

[8] G. W. McClure, Phys. Rev. 124, 969 (1961); G. W. McClure and K. D. Granzow, *ibid*. 125, 3 (1962); K. D. Granzow and G. W. McClure, *ibid*. 125, 1792 (1962).

[9] The ion source consisted of a cylindrical stainless steel anode 2 in. long and 0.750 in. in inside diameter. In each end of the anode was inserted a stainless steel cathode disk 0.625 in. in diameter. The cathodes were connected to a common source of potential about 500 V negative with respect to the anode. One of the cathodes was perforated by a central 0.020-in. aperture through which positive ions were extracted axially into the accelerator. An axial magnetic field of about 300 G was maintained within the ion source by a solenoid wrapped around the anode cylinder. The ion source discharge was usually operated at a current of the order of 10 μA.

[10] Chamber T$_1$ is intended for use as a charge-exchange chamber to make neutral beams and D$_1$ is primarily intended for stripping out residual ions when T$_1$ is used for this purpose. Neither T$_1$ nor D$_1$ was essential in the present work; however, D$_1$ was often used to check for the presence of "background" neutrals in the beam entering S$_3$ by making detector scans of the neutral beam from S$_4$ with the primary ion beam deflected off axis at D$_1$.
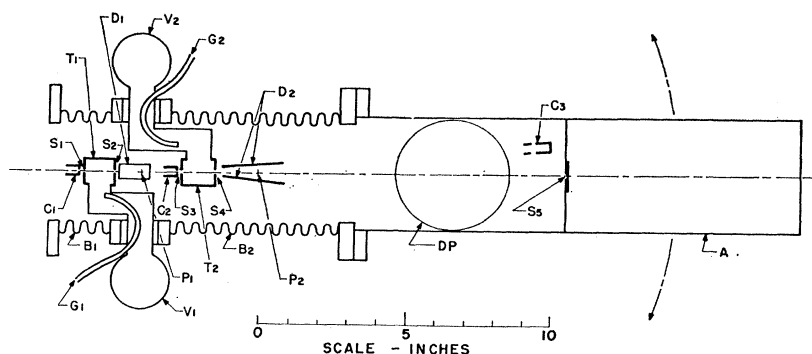
FIG. 1. Apparatus diagram. T_1 and T_2, collision chambers. V_1 and V_2, ionization gauges. G_1 and G_2, gas inlets. C_1, C_2, and C_3, Faraday cups. D_1 and D_2, deflection plates for deflecting charged particle beams off the main beam axis. S_1, S_2, S_3, and S_4, circular apertures having diameters 0.01, 0.02, 0.01, and 0.10 in., respectively. S_5, rectangular detector slit 0.001 in.$\times$0.963 in.; long dimension perpendicular to plane of drawing. A, ionization chamber forming lower section of counter assembly shown in Fig. 2. DP, 400 liter/sec oil diffusion pump. B_1 and B_2, bellows-type vacuum joints constrained by external gimbals. B_1 is used to align apertures S_1 and S_3 with direction of primary beam incident on S_1 from the left. B_2 is used for mechanically sweeping detector slit S_5 across the electrostatically analyzed set of particle beams emergent to the right from D_2. B_2 permits detector slit S_5 (and attached assemblies A and DP) to swing through a $\pm 20°$ arc in the plane of the drawing about center of rotation P_2. Cup C_3 is used to measure the primary ion beam emergent from S_4.

The present apparatus is somewhat similar to that of Schmid; however, several important differences should be noted: (1) Our use of a long slit, instead of a pinhole counter aperture as used by Schmid, eliminates the need for two-dimensional scanning of the secondary particle beams. (2) The present arrangement avoids electrostatic deflection of the primary ion beam as a part of the secondary beam scanning system. This makes possible the analysis of collision products from *neutral* primary beams without changing the apparatus. (3) The "collision region" (interior of T_2) has a well-defined length and is located relatively remotely from detector slit S_5. This makes possible the determination
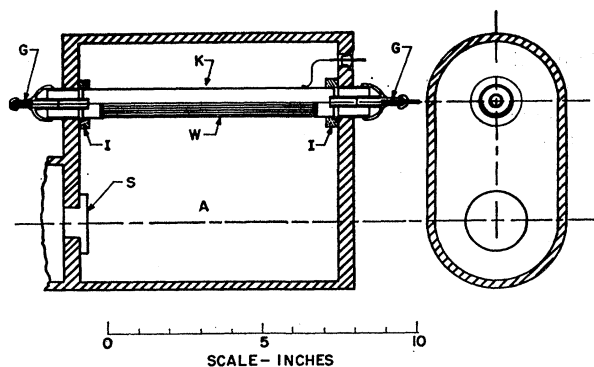

FIG. 2. Detector diagram. S, detector entrance slit (labeled S_5 in Fig. 1). A, ionization chamber. K, cylindrical cathode of proportional counter. W, grid forming lower half of cathode cylinder. I, insulating supports for cathode. The proportional counter anode is a 0.005-in.-diam tungsten wire on the axis of K. G, guard rings at anode potential. The detector assembly is operated with a methane gas filling at a pressure of 1.5 mm Hg. The slit S is covered with a collodion window (estimated thickness 0.5 μg/cm^2) which prevents the methane from passing into the high-vacuum system. Typical operating potentials: outer walls of A grounded, K at $+150$ V relative to ground, counter anode and guard rings at $+800$ V relative to ground. The detector output signal is developed across a 10^6 Ω load resistor connected between the $+800$ V supply potential and the anode wire.

of angular distributions of the collision fragments to scattering angles of $3°$. (4) The secondary ion beams are physically separated from the primary beams and each charged beam is counted separately in our apparatus. This completely eliminates the need of utilizing small differences in measured count rates for the determination of secondary ion production. (5) The relatively low-operating pressure of the present counter affords the use of comparatively thin entrance windows. This results in decreased proton scattering and reduced energy loss in the window. These factors tend to improve counter performance by reducing the statistical spread in pulse height. The resolution of the counter is illustrated by the pulse-height distributions shown in Fig. 3. At H_2^+ energies above 10 keV, the separate peaks due to H and H_2 secondaries are well resolved. Between 10 and 3 keV, the composite H, H_2 distributions can be fairly easily resolved by statistical analysis using pulse-height distributions from "pure" beams of H^+ and H_2^+ to determine the individual peak shapes. The counter has identical response to H atoms and H^+ ions of the same energy. H_2 molecules and H_2^+ ions of the same energy are assumed to give identical distributions.[11]

MEASUREMENT PROCEDURE

Cross sections were determined from the working formulas:

$$\sigma_i = (I_i/I_0)(1/nd),$$

$$I_i = C_i v/w,$$

$$n = ap,$$

[11] This cannot be checked exactly because there is no way of obtaining a pure H_2 beam with the present apparatus. It is practically certain that either H_2^+ or H_2 particles dissociate after passing through a few atom layers of the entrance window and that the mean free paths for proton electron capture and loss are short compared to the window thickness. Hence, by the time the dissociation fragments of a primary molecular particle reach the counter interior there is no correlation between the charge of the entering particle and the charge state of its dissociation fragments.
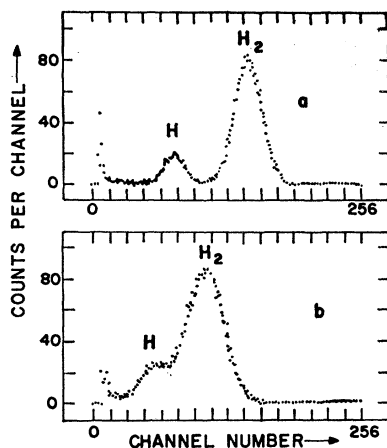
FIG. 3. Pulse-height distribution (256 channel) of detector output pulses recorded with detector slit set on center of neutral beam emerging from collision chamber. a, recording with 10-keV primary H_2^+ ions entering collision chamber. b, recording with 5-keV primary H_2^+ ions entering collision chamber. Peaks labeled H_2 are due to H_2^+ ions neutralized by electron capture. Peaks labeled H are due to H atoms from dissociation of H_2^+ ions. At primary H_2^+ energies greater than 10 keV, H and H_2 peaks are completely separated. At and below 10 keV, corrections were made for peak overlap in calculating the partial yields of H and H_2.

where σ_i= cross section for production of secondary particle of type i, I_0= current of primary particles, I_i= current of secondary particles of type i, n= density of gas molecules in collision chamber, d= effective length of collision chamber, C_i= number of counts from secondaries of type i recorded during one detector scan across the type-i beam, v= velocity of scanning motion of slit S_5, w= width of slit S_5 in direction of scanning motion, p= collision chamber relative pressure as measured by ionization gauge G_2, and a= calibration constant relating n and p. The above formulas may be combined to give

$$\sigma_i = (C_i/pI_0)(v/wad),$$

where the quantity v/wad is the over-all calibration constant of the apparatus. This constant was determined by measurement of C_i/pI_0 for electron capture by 10-keV H^+ ions and by the assumption of the value $\sigma_i = 8.2 \times 10^{-16}$ cm² for the electron capture process.[12] Measurements of the calibration constant were made at frequent intervals throughout the data runs to make sure that all measuring equipment was remaining stable. Variations of $\pm 5\%$ from the mean were observed in a large number of determinations over several months' time. These variations were attributable to counting statistics, to errors, in reading p and I_0, and to small variations in v.

A rough calculation of the calibration constant v/wad, gotten by using estimated values of v, w, a, and d, agreed within 15% with the value obtained as described above. The consistency appeared to be satis-

factory in view of uncertainties of about 10% in the values of a, w, and d. With some care, both a and w could have been determined with much greater precision. The only real problem in a precise absolute calibration would be in determining d accurately. This would involve a careful calculation of the collision chamber pressure profile. Such a calculation has not been attempted for the present collision chamber geometry.

The gas pressure in the collision chamber was maintained at a level sufficiently low that, at most, 1% of the primary ions was absorbed. The pressures in the drift spaces before and after the collision chamber were of the order of 100 times lower than the collision chamber pressure. Hence, neither the primary beam particles nor the secondaries produced in the collision chamber were appreciably absorbed or altered by drift-space collisions.

In *every individual* cross-section measurement a curve of C_i/I_0 versus p was taken to insure that a linear relationship existed between these two quantities. These curves were run over a pressure range of 10^{-5} to 10^{-4} mm Hg and the curves were always linear within experimental error; however, in some cases the curves extrapolated to C_i/I_0 values significantly greater than zero at $p=0$. In any such case the slope of the curve was used to determine the value of $C_i/I_0 p$ needed in evaluating the cross section. This procedure removed any background due to residual gas in the collision chamber, production of the secondary particles at the edges of slit S_3, or production of secondaries in the drift space ahead of S_3. In no case was the extrapolated value of C_i/I_0 at $p=0$ more than one-tenth the C_i/I_0 value at 10^{-4} mm Hg.

In all measurements of C_i on each secondary-particle beam, detector slit S_5 was scanned a distance of 1 in. perpendicular to its long dimension. Thus, the effective detector "window" was a rectangle 0.963 in.$\times$1 in. at a distance of 12.5 in. from the center of the collision chamber. In each case, the "window" was carefully centered on the secondary-particle beam being measured. Under these conditions the detector received all particles of a given type produced within a 2.2° angle of the collision chamber axis. Angular distributions of the various collision products were taken at the lowest and highest primary beam energies (5 and 100 keV) by recording count rate versus position of slit S_5 during a standard 1-in. scan. In all cases the count rates were down at least one order of magnitude at the edges of the scan as compared with the peak value at the center of the scan. Figure 4 shows a typical automatic plot of count rate versus position of slit S_5.

RESULTS

H⁺ Primaries

The cross section σ_H for conversion of H^+ ions to neutral H atoms is shown in Fig. 5. The value of the

[12] S. K. Allison and M. Garcia-Munoz, in *Atomic and Molecular Processes*, edited by D. R. Bates (Academic Press Inc., New York, 1962), p. 751.
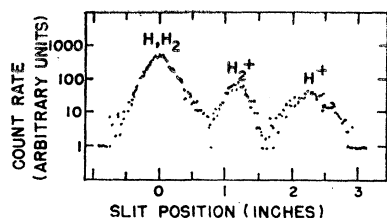
FIG. 4. Plot of detector count rate vs displacement of detector slit S_5 for 6-keV H_3^+ primaries showing neutral and charged secondaries from the collision chamber resolved into separate beams. The primary H_3^+ beam did not register because it was being intercepted by cup C_3. (In the absence of the cup, the primary beam would have appeared as a very strong and very narrow peak at the $\frac{3}{4}$-in. slit position.) The slight asymmetry of the neutral (H, H_2) beam is believed to be due to a small contribution on the right-hand side due to elastically scattered primary H_3^+ ions or dissociation fragments produced in the residual gas in the high-vacuum drift space beyond S_4. This pattern represents the "worst" case of spacial resolution of collision products in the present experiments. The secondary particle beam widths were narrower at higher energies and were narrower for H_2^+ and H^+ primaries of a given energy than for H_3^+ primaries.

calibration constant was chosen so as to normalize the measured cross section at 10 keV to the mean of several closely agreeing absolute measurements at 9 and 11 keV tabulated in a recent review article.[12] With the same normalization, all measured σ_H values between 3 and 100 keV fit within a few percent of a curve based upon the averaged results of other workers over this same energy range. This close fit gave assurance that no significant systematic errors were present in the measuring technique and that the proportional counter detector had no decrease in efficiency at low energies due to stopping or backscattering in the counter entrance window.

H_2^+ Primaries

Experimental results for H_2^+ primaries are shown in Fig. 6. σ_H, σ_{H_2}, and σ_H^+ are, respectively, the cross
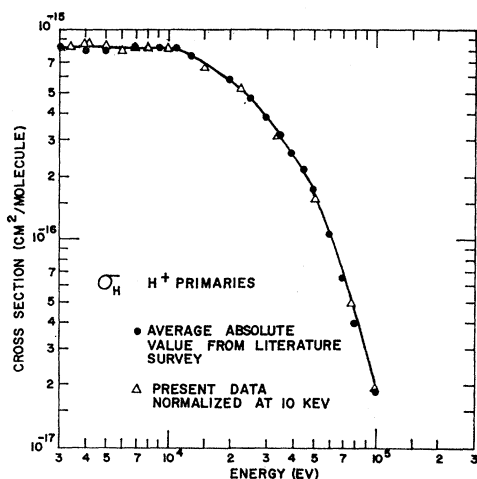

FIG. 5. Cross section for conversion of H^+ ions into neutral H atoms.

TABLE I. Dependence of measured cross sections on ion-source gas pressure. H_2^+ primary ions, 10-keV beam energy, cross-section units $= 10^{-16}$ cm^2.

Pressure	σ_H	σ_{H_2}	σ_H^+
15μ	7.28±0.20	4.60±0.16	2.42±0.12
50μ	7.28±0.19	4.20±0.14	1.90±0.10

sections for production of H atoms, H_2 molecules, and H^+ ions having essentially the same velocity as the primary H_2^+ ions. The ion source was operated at a pressure of 10 to 15 μ (H_2 gas) in all measurements and the analyzer magnet and accelerator controls were adjusted so that ions from the peak of the ion-source energy spectrum were employed. Successive determinations of cross-section values were found to scatter about ±10% from the mean. The scatter was satis-
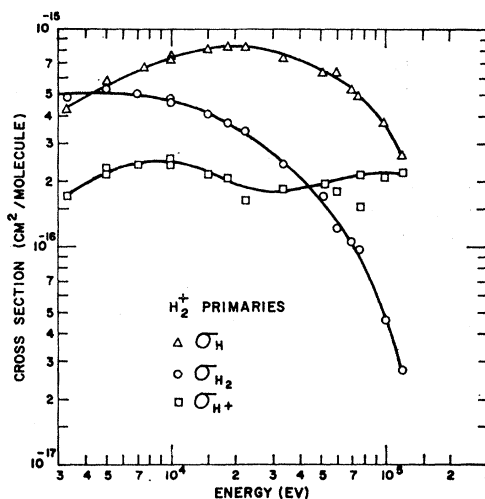

FIG. 6. Cross sections for conversion of primary H_2^+ ions into heavy secondaries. σ_H, σ_{H_2}, and σ_H^+ are, respectively, the production cross sections of H, H_2, and H^+ secondaries having essentially the same velocity as the primary ions.

factorily accounted for by estimated errors in the pressure readings, beam current readings, and particle counts.

When the ion-source gas pressure was varied from 15 to 50 μ with a beam energy of 10 keV, the cross sections measured were as shown in Table I. The reduction in σ_H^+ with increasing source pressure was considered to be well outside the experimental errors and was reproduced in several trials.

In the above test the accelerator was adjusted, as on the regular runs, to the peak of the ion source energy spectrum. In another series of tests the pressure was kept constant at 15 μ while the accelerator high voltage was raised about 200 V from the value required to give peak output current. This test also was performed at a net ion energy of 10 keV. Results are shown in Table II. In this case no significant change was introduced in

TABLE II. Dependence of measured cross sections on portion of ion-source energy spectrum from which ions were selected. H$_2$$^+$ primary ions, 10-keV beam energy, cross-section units $= 10^{-16}$ cm^2.

Origin of ions	σ_H	σ_{H_2}	$\sigma_H{}^+$
Peak of source spectrum	7.39±0.22	4.66±0.17	2.30±0.12
Low-energy side of source spectrum peak	5.78±0.28	4.66±0.25	1.89±0.10

σ_{H_2} but both σ_H and $\sigma_H{}^+$ were substantially altered. Careful rechecks of these tests left no doubt that the susceptibility of the ions to collisional dissociation depended on both the energy of emission of the ions from the source and the pressure of the source gas. The basic physical effect involved appears to be that H$_2$$^+$ ions are produced within the ion source in various excited states, the population of such states being variable with the pressure and the distance the ions travel in the electric field before leaving the extraction aperture of the ion source.
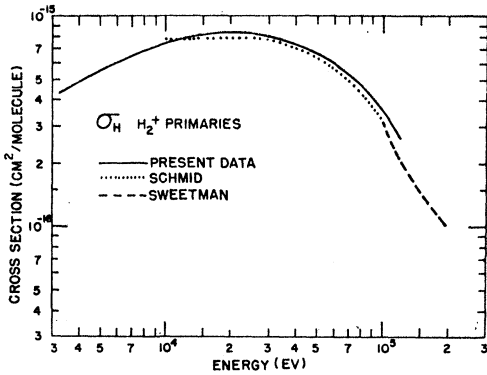

FIG. 7. Comparison of present data on σ_H for H$_2$$^+$ primaries with data of Schmid (reference 6) and Sweetman (reference 4).

The results plotted in Fig. 6 are compared with results of other investigations in Figs. 7, 8, and 9. The present σ_H and σ_{H_2} results agree with the results of Schmid[6] and Sweetman[4] within 20% at all energies from 10 to 120 keV. This agreement appears to be satisfactory in view of the probable errors in the respective measurements, and particularly in view of our finding that changes in ion source operating conditions can introduce systematic changes of at least 10% in σ_{H_2} and 20% in σ_H.

The spread in the various measurements of $\sigma_H{}^+$ (Fig. 9) is a great deal larger than the spread in the σ_H and σ_{H_2} measurements. The $\sigma_H{}^+$ results based on measurements of the secondary H$^+$ ion beam by means of Faraday cups (Damodaran,[1] Fedorenko,[3] and Barnett[2]) are very widely divergent from one another and fall both above and below the present results. On the other hand, the group of measurements in which counters or scintillation detectors were used to detect the H$^+$ ions (Schmid,[6] Sweetman,[4] Guidini[5]) are in relatively close
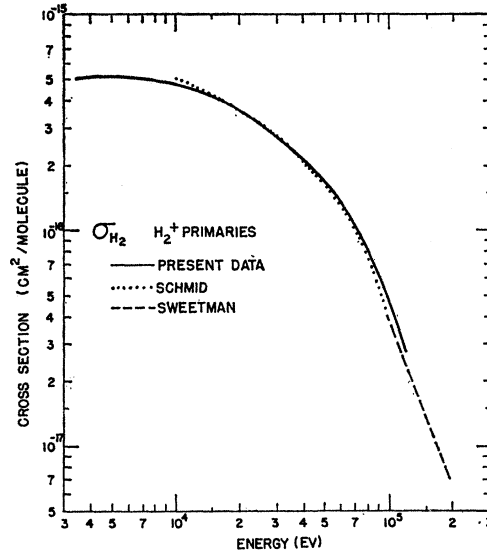

Fig. 8. Comparison of present data on σ_{H_2} for H$_2$$^+$ primaries with data of Schmid (reference 6) and Sweetman (reference 4).

mutual agreement and diverge relatively little from the present results. Considering both random experimental errors and the possibility of 10 to 20% discrepancies due to differences in ion source operating conditions, it is barely possible to reconcile all of the $\sigma_H{}^+$ measurements which used counters as detectors. The unexplained large divergencies of the Fedorenko and Barnett results from the mean of the "counter" results may be due, in part, to the collection of spurious currents of slow particles in the Faraday cups used to detect the H$^+$ beams in those experiments. The use of energy sensitive particle detectors aids greatly in eliminating this source of error.

In the present experiments we have not explored the full gamut of possible variations in cross sections that
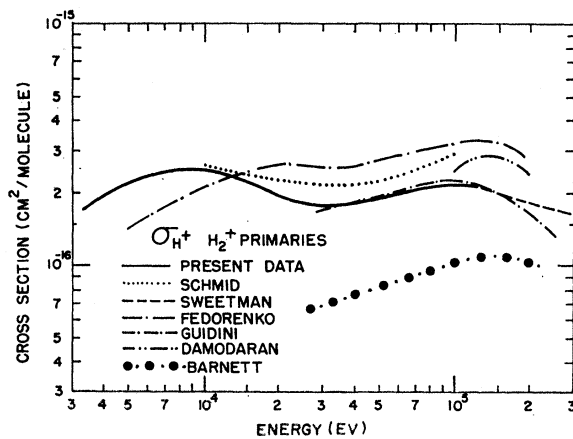

FIG. 9. Comparison of present data on $\sigma_H{}^+$ for H$_2$$^+$ primaries with data of Schmid (reference 6), Sweetman (reference 4), Fedorenko (reference 3), Guidini (reference 5), Damodaran (reference 1), and Barnett (reference 2).
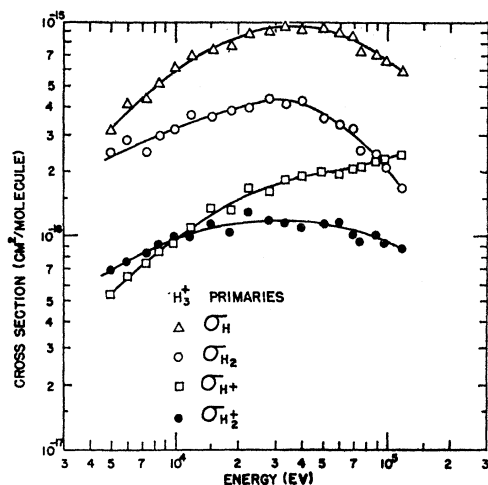
FIG. 10. Cross sections for conversion of primary H_3^+ ions into heavy secondaries. σ_H, σ_{H_2}, σ_H^+ and $\sigma_{H_2}^+$ are, respectively, the production cross sections of H, H_2, H^+, and H_2^+ secondaries having essentially the same velocity as the primary ions.

may arise from differences in ion sources and ion source operating conditions. Further work on this subject is very desirable.

H_3^+ Primaries

Experimental results for H_3^+ primaries are shown in Fig. 10. σ_H, σ_{H_2}, σ_H^+, and $\sigma_{H_2}^+$ are, respectively, the cross sections for production of H atoms, H_2 molecules, H^+ ions, and H_2^+ ions having essentially the same velocity as the primary H_3^+ ions. The ion source operating conditions were the same as those used in obtaining the data for H^+ and H_2^+ primaries.

The cross sections σ_H, σ_{H_2}, and $\sigma_{H_2}^+$ all pass through relative maxima at primary ion energies of 30–40 keV, but the σ_H^+ cross section increases monotonically with energy at least up to 120 keV. A comparison of Figs. 6 and 10 shows that H_2^+ and H_3^+ ions both have dissociation cross sections of the order of 10^{-16} to 10^{-15} cm^2 over the energy range investigated.

No evidence whatever was found for a stable H_3 neutral molecule produced by H_3^+ ion neutralization. The presence of the H_3 species in the fast neutral beam would have been detected if its production were as great as 1% of the H_2 neutral molecule production.

Investigations of the effect of ion source settings on the H_3^+ cross sections were conducted as in the case of the H_2^+ cross sections. Using H_3^+ primary ions of 15-keV energy the cross sections were found to depend on source gas pressure as shown in Table III. A definite

TABLE III. Dependence of measured cross sections on ion-source gas pressure. H_3^+ primary ions, 15-keV beam energy, cross-section units $= 10^{-16}$ cm^2.

Pressure	σ_H	σ_{H_2}	σ_H^+	$\sigma_{H_2}^+$
14μ	6.97±0.07	3.32±0.05	1.26±0.04	1.08±0.04
55μ	6.04±0.09	3.05±0.06	1.02±0.04	0.84±0.03

decrease in the cross sections correlated with increase in source pressure appears to be present. It is believed that this effect is associated with a change in the population of excited states of the H_3^+ ions.

INTERNAL ENERGY STATES OF H_2^+ AND H_3^+ IONS

In the preceding section of this paper evidence was shown of a dependence of the measured dissociation cross sections on the ion-source gas pressure and the kinetic energy of emergence of the ions from the ion source. It was suggested that this dependence was associated with a variable population of excited states of the ions. This hypothesis is now examined in somewhat more detail using a classical model of the interaction of molecular ions and gas molecules to show how ions may become excited in the ion source. We consider in particular the colliding system H_2^+ and H_2 and assume that the primary ion, H_2^+, has a kinetic energy of 200 eV. This energy is fairly typical of the energies of the ions emergent from the ion source.

Using the classical impulse approximation to examine the interaction between one of the fast moving protons of the "incident" H_2^+ ion and one of the protons of the "target" H_2 molecule, it is easily shown that proton-proton energy exchanges of 2 eV or more occur with an effective cross section of about 10^{-15} cm^2. Such energy exchanges would result in violent vibrational and rotational excitation of both the H_2^+ ion and the target H_2 molecule, and would occur with a mean free path of about 2 cm at a pressure of 15 μ H_2. The process should then be an important one in our ion source and should vary in probability as the source pressure is varied over the range of these experiments (15–50 μ).

There are at least three ways in which H_2^+ ions may be produced in the Penning-type ion source: (1) by direct electron impact ionization of H_2, (2) by dissociation of H_3^+ ions, and (3) by charge-exchange collisions in which H_2^+ ions are formed from neutral gas molecules by electron exchange with H_3^+, H_2^+, and H^+ ions. It should be mentioned that the yield of H^+ and H_3^+ ions from the ion source was very low compared to the yield of H_2^+. However, it is possible that the discharge contains a plasma region near the anode in which H_3^+ ions predominate.[13] In this case many of the H_2^+ ions which enter the exit aperture region would be products of H_3^+ ion dissociation. The important point to note is that H_2^+ ions produced in the three types of processes mentioned are very likely to possess different vibrational and rotational energy distributions and the relative abundance of ions from the three origins at the exit aperture is undoubtedly pressure dependent as well as ion-energy dependent.

The known electronically excited bound states of the H_2^+ ion[14] ($2p\pi_u$ and $3d\sigma_g$) are very weakly bound (0.25

[13] R. N. Varney, Phys. Rev. Letters **5**, 559 (1960); W. S. Barnes, D. W. Martin, and E. W. McDaniel, *ibid.* **6**, 110 (1961).

[14] D. R. Bates, K. Ledsham, and A. L. Stewart, Phil. Trans. Roy. Soc. (London) **A246**, 215 (1953).

and 1.36 eV, respectively), and the minima of the molecular potentials for these excited states are greatly displaced from the minima of the H$_2$ molecule and H$_2$$^+$ ion ground states. Application of the Frank-Condon principle under these circumstances indicates that electronic excitation of H$_2$$^+$ would lead directly to dissociation. It is, therefore, felt that the ion-source effect observed for H$_2$$^+$ ions is due to vibrational or rotational excitation rather than to electronic excitation of the primary ions. The properties of excited electronic states of H$_3$$^+$ are not well known but an impulse argument for a high cross section for vibrational and rotational excitation in the ion source probably holds for H$_3$$^+$ ions as well as for H$_2$$^+$ ions.

It is practically certain that the dissociation cross sections of H$_2$$^+$ and H$_3$$^+$ ions in the high-energy collisions studied herein are affected by vibrational and rotational excitation of the type discussed above. If one applies the same impulse argument as was used above to calculate the cross section for 2-eV proton excitations of molecular ions in 10-keV collisions, the cross section comes out to be much smaller ($\sim$50 times smaller) than for 200-eV ions. This makes the proton impact contribution to the total cross section about 2×10^{-17} cm^2, which is smaller than the observed H$_2$$^+$ and H$_3$$^+$ dissociation cross sections. It would, therefore, appear that the high-energy dissociations of H$_2$$^+$ and H$_3$$^+$ occur by a process of electronic excitation.

It is worth noting that the energy separation between the $^2\Sigma_g$ and $^2\Sigma_u$ states of the H$_2$$^+$ ion is a rapidly varying function of the nuclear separation. In highly excited vibrational states the molecular ion spends a relatively large amount of time with its two protons far apart where the electron energy difference between the bonding and antibonding $^2\Sigma_g$ and $^2\Sigma_u$ states is very small. It might, therefore, be expected that the transition probability to the antibonding state is greatly increased by vibrational excitation. In this case the dissociation probabilities of the high-energy ions would be strongly affected by the states in which the ions are prepared in the ion source.

CONCLUSIONS

The present method of measuring the dissociation cross sections of fast H$_2$$^+$ and H$_3$$^+$ ions is capable of giving relative cross sections accurate to a few percent. We have not pressed the present measurements to this degree of accuracy because of our discovery that the measurements depend on the ion source settings. This dependence appears to be associated with the excitation of internal vibrational and rotational states in the primary molecular ions before these ions leave the ion source. Further refinements in experimental determinations of molecular ion cross sections depend upon the development of means of controlling or determining the excited state population of the primary ions.

Note added in proof. In discussing prior related work, the author inadvertently overlooked the work of Fedorenko on H$_3$$^+$ dissociation in which the yields of secondary fast H$_2$$^+$ and H$^+$ ions were measured for H$_3$$^+$ primary ions of 5 to 25 keV [N. V. Fedorenko, Zh. Tekhn. Fiz. **24**, 769 (1954)]. These results tend toward close agreement with the present results at 25 keV, but fall below the present results by about a factor of two at 5 keV. The discussion in reference 3 suggests that some of the larger angle dissociation fragments may have been undetected in the 1954 Fedorenko measurements. This would tend to explain the facts that the 1954 Fedorenko cross sections are, in general, lower than ours, that the agreement of the H$_2$$^+$ production cross sections is closer than that of the H$^+$ production cross sections, and that the agreement is better at higher energies.